Biodegradation (2011) 22:51–61
DOI 10.1007/s10532-010-9375-7

ORIGINAL PAPER

Anchorage of GFP fusion on the cell surface of *Pseudomonas putida*

Yulan Yuan · Chao Yang · Cunjiang Song · Hong Jiang · Ashok Mulchandani · Chuanling Qiao

Received: 19 March 2010 / Accepted: 25 May 2010 / Published online: 16 June 2010

Abstract Here we report the cell surface display of organophosphorus hydrolase (OPH) and green fluorescent protein (GFP) fusion by employing the N- and C-terminal domains of ice nucleation protein (INPNC) as an anchoring motif. An *E. coli–Pseudomonas* shuttle vector, pNOG33, coding for INPNC–OPH–GFP was constructed for targeting the fusion onto the cell surface of *p*-nitrophenol (PNP)-degrading *P. putida* JS444. The surface localization of INPNC–OPH–GFP was verified by cell fractionation, Western blot, proteinase accessibility, and immunofluorescence microscopy. Furthermore, the functionality of the surface-exposed OPH–GFP was demonstrated by OPH assays and fluorescence measurements. Surface display of macromolecular OPH–GFP fusion (63 kDa) neither inhibited cell growth nor affected cell viability. These results suggest that INP is an useful tool for the presentation of heterologous proteins on cell surfaces of indigenous microbes. The engineered *P. putida* JS444 degraded organophosphates (OPs) as well as PNP rapidly and could be easily monitored by fluorescence. Parathion (100 mg kg^{-1}) could be degraded completely within 15 days in soil inoculated with the engineered strain. These merits make this engineered strain an ideal biocatalyst for in situ bioremediation of OP-contaminated soil.

Keywords Surface display · Organophosphorus hydrolase · Green fluorescent protein · Ice nucleation protein · *Pseudomonas putida*

Yulan Yuan and Chao Yang contributed equally to this work.

Electronic supplementary material The online version of this article (doi:10.1007/s10532-010-9375-7) contains supplementary material, which is available to authorized users.

Y. Yuan · H. Jiang · C. Qiao (✉)
State Key Laboratory of Integrated Management of Pest Insects and Rodents, Institute of Zoology, Chinese Academy of Sciences, Beijing 100101, China
e-mail: qiaocl@ioz.ac.cn

C. Yang · C. Song
Department of Microbiology, College of Life Sciences, Nankai University, Tianjin 300071, China
e-mail: yang_chao2008@hotmail.com

A. Mulchandani (✉)
Department of Chemical and Environmental Engineering, University of California, Riverside, CA 92521, USA
e-mail: adani@engr.ucr.edu

Introduction

Synthetic organophosphates (OPs) are widely used to control various agriculture pests and account for ~38% of the total pesticides used globally (Singh and Walker 2006). In the United States alone, over 40 million kg of OP pesticides are consumed

annually (Shimazu et al. 2001b). OPs are acute neurotoxins by virtue of their potent inhibition of acetylcholinesterase (AChE), and various clinical effects can occur from OP poisoning in humans (Sogorb et al. 2004).

Organophosphorus hydrolase (OPH), isolated from *Pseudomonas diminuta* MG and *Flavobacterium* sp. strain ATCC 27551, is a zinc-containing homodimeric protein that has a broad substrate specificity with an ability to hydrolyze P–O, P–F, and P–S bonds (Serdar and Gibson 1985; Mulbry et al. 1986). The rates of hydrolysis by OPH differ dramatically for members of the family of OPs, ranging from hydrolysis at the diffusion-controlled limit for paraoxon to several orders of magnitude slower for malathion, chlorpyrifos, and VX (Dumas et al. 1989; Raushel 2002). Hydrolysis of OPs by OPH reduces their toxicity by several orders of magnitude (Sogorb et al. 2004). However, practical applications of large-scale enzymatic degradation have always been limited by the cost of purification and stability of OPH. Although the use of natural isolates as biocatalysts is an alternative strategy for treatment of OPs, the inaccessibility of OPs across the cell membrane reduces the overall catalytic efficiency (Richins et al. 1997). This bottleneck, however, could be eliminated if OPH is displayed on the cell surface (Richins et al. 1997; Shimazu et al. 2001a, b; Lei et al. 2005). Periplasmic secretion of OPH via the Tat system can be an alternative strategy for alleviating the substrate uptake limitation (Kang et al. 2005).

An OP-hydrolyzing enzyme, OpdA, has been isolated from *Agrobacterium radiobacter* and was found to have 90% homology to OPH at the amino acid level (Horne et al. 2002), and there is a commercially available in situ bioremediant based upon OpdA called LandGuard. In 2001, an OP degradation gene (*mpd*) encoding methyl parathion hydrolase (MPH) was isolated from *Plesiomonas* sp. strain M6, but it lacks sequence homology with the *opd* gene that encodes OPH (Cui et al. 2001). In particular, OPH and MPH have different substrate specificities. OPH has high hydrolytic activity with numerous diethyl OPs, while MPH has a higher k_{cat}/K_m value for dimethyl OPs than OPH (Dumas et al. 1989; Cui et al. 2001). Previously, we cloned the *mpd* gene from *Stenotrophomonas* sp. strain YC-1 and, furthermore, MPH was functionally displayed on the cell surface of *P. putida* JS444 (Yang et al. 2006, 2008).

Ice nucleation protein (INP) is an outer membrane protein from *P. syringae*, which accelerates ice crystal formation in supercooled water. INP has a multidomain organization with an N-terminal domain containing three or four transmembrane spans, a C-terminal domain, and a highly repetitive central domain for ice nucleation (Kozloff et al. 1991; Wolber 1993). INP has been successfully used to display heterologous proteins, such as levansucrase (Jung et al. 1998a), carboxymethylcellulase (Jung et al. 1998b), salmobin (Jeong et al. 2001), OPH (Shimazu et al. 2001a), and GFP (Li et al. 2004), on the cell surface of *E. coli*. INP-mediated cell surface display can be achieved using either full-length INP sequences or truncated INP sequences (Jung et al. 1998a, b; Shimazu et al. 2001a; Li et al. 2004). INP is well suited as a carrier of larger proteins, such as 60 kDa HIV-1 gp120 (Kwak et al. 1999), 77 kDa cytochrome P450 oxidoreductase (Yim et al. 2006), and 90 kDa chitinase (Wu et al. 2006).

In order to develop a bioremediation technology for in situ application of the organism, it is important to design a monitoring method for determining its movement in the environment and also to evaluate the risk factor and performance of the organism during the bioremediation process (Prosser 1994). In the past few years, there has been continuous development in methods for tracking microorganisms deliberately released in the environment with an emphasis on increased sensitivity and specificity (Larrainzar et al. 2005; Xu 2006). These methods include phenotype-based methods and also DNA-based molecular methods.

The phenotype-based methods focus on the use of stable marker systems with an easily detectable phenotype. Green fluorescent protein (GFP) requires no cofactors or substrates for its fluorescence and can be detected noninvasively using fluorescence microscopy and flow cytometry (Chalfie et al. 1994). Moreover, GFP can be expressed as either an N- or C-terminal fusion (Tsien 1998; Cha et al. 2000). In ecological studies, GFP can be used as a marker to assess survival and activity of microbes (Errampalli et al. 1999; Elväng et al. 2001; Larrainzar et al. 2005).

Recently, a recombinant *E. coli* strain was genetically engineered to coexpress OPH and MPH, and it has a broader substrate range than strains expressing either one of the hydrolases (Yang et al. 2010).

However, *E. coli* strains are not suitable for in situ remediation since they are not adapted to these environments. A more realistic approach is to engineer soil bacteria that are known to survive in contaminated environments for an extended period. Walker and Keasling (2002) engineered *P. putida* KT2442 to use parathion as a source of carbon and energy. Many species of the genus *Pseudomonas* are robust and ubiquitous in soils and are capable of degrading a wide variety of pollutants.

p-Nitrophenol (PNP), a byproduct from OP hydrolysis that is stable and toxic to humans. PNP is still classified as a priority pollutant by the U.S. EPA (Shimazu et al. 2001b). *P. putida* JS444 is particularly attractive as it was isolated from PNP-contaminated waste sites and can rapidly degrade PNP (Nishino and Spain 1993). In the present study, OPH–GFP fusion was displayed on the cell surface of *P. putida* JS444 using the truncated InaV protein. The engineered strain was endowed with the capability to degrade OPs and PNP and could potentially be tracked by fluorescence during bioremediation.

Materials and methods

Bacterial strains, plasmids, and culture conditions

All strains, plasmids, and primers used in this study are listed in Table 1. *E. coli* DH5α was used for constructing recombinant plasmids. *P. putida* JS444 was used as host strain for cell surface display of OPH–GFP. Strains bearing plasmids were grown in Luria–Bertani (LB) medium (Sambrook and Russel 2001) or minimal salts medium (Spain and Nishino 1987) supplemented with kanamycin to a final concentration of 50 μg ml^{-1}. Expression of INPNC–OPH–GFP was induced with 0.2 mM isopropyl-*β*-D-thiogalactopyranoside (IPTG) when cells were grown to an optical density at 600 nm (OD_{600}) of 0.4. After IPTG induction, cells were incubated at 30°C for 24 h.

Plasmid construction

The *inpnc–opd* fusion gene was PCR amplified from pPNCO33 (Shimazu et al. 2001b) using primers P1

Table 1 Strains, plasmids and primers used in this study

Strain, plasmid or primer	Description[a]	Source or reference
Strains		
E. coli DH5α	*supE44* Δ*lacU169*(*φ80 lacZ*ΔM15) *recA1 endA1 hsdR17*(r_K^- m_K^+) *thi-1 gyrA relA1* F^- Δ(*lacZYA-argF*)	Tiangen
P. putida JS444	A natural PNP degrader	Nishino and Spain (1993)
Plasmids		
pPNCO33	Source of *inpnc–opd* fusion gene	Shimazu et al. (2001b)
pEGFP-N3	Source of *gfp* gene	Cormack et al. (1996)
pVLT33	*E. coli–Pseudomonas* shuttle vector, *oriT*, RSF1010, *oriV*, $lacI^q$, *tac* promoter, Km^r	de Lorenzo et al. (1993)
pNOG33	pVLT33 derivative, surface expression vector coding for INPNC–OPH–GFP fusion	This study
pOG33	pVLT33 derivative, control plasmid for expressing cytosolic OPH–GFP fusion	This study
Primers		
P1	GAATTCAGGAAACAATGAATATCGACAAAGCGTTGGTA	This study
P2	GGATCCTGACGCCCGCAAGGTCGGTGA	This study
P3	GGATCCATGGTGAGCAAGGGCGAG	This study
P4	AAGCTTTTACTTGTACAGCTCGTCCA	This study
P5	GAATTCAGGAAACAATGCAAACGAGAAGGGTTGTGCTC	This study

[a] The restriction sites in the primers (5′ → 3′) are underlined

and P2, digested with *Eco*RI/*Bam*HI and ligated into similarly digested pVLT33 (de Lorenzo et al. 1993), an *E. coli–Pseudomonas* shuttle vector, to generate pNO33. The *gfp* gene was PCR amplified from pEGFP-N3 (Cormack et al. 1996) using primers P3 and P4, digested with *Bam*HI/*Hin*dIII and ligated into similarly digested pNO33 to generate pNOG33.

The *opd–gfp* fusion gene was PCR amplified from pNOG33 using primers P5 and P4, digested with *Eco*RI/*Hin*dIII and ligated into similarly digested pVLT33 to generate pOG33. All plasmid constructions were verified by DNA sequence analysis. Transformation of plasmid into *P. putida* JS444 was carried out using the $CaCl_2$–$MgCl_2$ method (Lei et al. 2005).

Cell fractionation

Cells carrying pNOG33 were harvested and resuspended in 25 mM Tris–HCl buffer (pH 8.0). After disruption of the cells by sonication and a brief clarifying spin, the clarified lysate was ultracentrifuged at 50,000 rpm for 1 h at 4°C and the supernatant was retained as the soluble fraction. The pellet (total membrane fraction) was resuspended with PBS containing 0.01 mM $MgCl_2$ and 2% Triton X-100 for solubilizing the inner membrane and was incubated for 30 min at room temperature, and then the outer membrane fraction was repelleted by ultracentrifugation (Li et al. 2004; Lei et al. 2005).

SDS-PAGE and Western blot analysis

Subcellular fractionated samples were mixed with sample buffer (200 mM Tris–HCl pH 6.8, 8% SDS, 0.04% bromophenol blue, 8% β-mercaptoethanol, 40% glycerol), boiled for 5 min, and analyzed by 12% sodium dodecyl sulfate-polyacyrlamide gel electrophoresis (SDS-PAGE) (Sambrook and Russel 2001). Proteins were electroblotted onto nitrocellulose membranes using a tank transfer system (Bio-Rad) at 40 V for 3 h. Blotted membranes were blocked in TBST (20 mM Tris–HCl pH 7.5, 150 mM NaCl, 0.05% Tween-20) with 3% bovine serum albumin (BSA). For immunodetection, membranes were incubated with either OPH or GFP antiserum diluted (1:1,000) in TBST with 3% BSA for 3 h. After being washed with TBST, secondary antibody was added and incubated for 2 h at room temperature. Antigen–antibody conjugates were visualized by reaction with alkaline phosphatase-conjugated goat anti-rabbit IgG secondary antibody diluted (1:2,000) in TBST. After being washed with PBS, a color reaction was achieved by using the Immun-Blot BCIP/NBT kit (Bio-Rad).

Immunofluorescence microscopy

Cells were harvested and resuspended ($OD_{600} = 0.5$) in PBS with 3% BSA. Cells were then incubated with either OPH or GFP antiserum diluted (1:500) in PBS for 3 h at 30°C. After being washed with PBS, cells were resuspended in PBS with goat anti-rabbit IgG conjugated with rhodamine (1:100 dilution) and were incubated for 2 h at 30°C. Prior to microscopic observation, cells were washed five times with PBS and mounted on poly(L-lysine)-coated microscopic slides. Photographs were taken using a fluorescence microscopy (Nikon) equipped with FITC and Rhodamine filters.

OPH assay

Organophosphorus hydrolase activity was assayed with paraoxon by monitoring the increases in the absorbance at 405 nm ($\varepsilon_{405} = 17{,}700\ M^{-1}\ cm^{-1}$ for PNP) at 37°C using a Beckman DU800 spectrophotometer (Richins et al. 1997). For each assay, 200 µl of cells ($OD_{600} = 1.0$) were added to 700 µl of 50 mM citrate–phosphate buffer with 50 µM $CoCl_2$ (pH 8.0) and 100 µl of 20 mM paraoxon (Sigma) in 10% methanol. One unit (U) of activity was defined as the formation of 1 µmol PNP per min.

Fluorescence measurement

The GFP fluorescence intensity was determined using a fluorescence spectrophotometer (F-4500, HITACHI) with a bandwidth of 5 nm, an excitation wavelength of 488 nm, and an emission wavelength of 510 nm. Cells were resuspended ($OD_{600} = 1.0$) in PBS buffer (pH 7.5) and assayed for fluorescence. The fluorescence signal of the untransformed cells was set as background and was subtracted from the overall fluorescence.

Proteinase accessibility assay

Cells were harvested and resuspended ($OD_{600} = 10$) in PBS buffer (pH 7.5). Pronase (4 U mg^{-1}; Sigma)

was added to a final concentration of 2 mg ml^{-1}. Cell suspensions were incubated at 37°C for 3 h. Pronase treated and untreated cells were assayed for OPH activity and GFP fluorescence.

Stability study of resting cultures

Cells with surface-displayed OPH–GFP were resuspended in 5 ml of 50 mM citrate–phosphate buffer (pH 8.0) with 50 μM $CoCl_2$ and incubated in a shaker at 30°C. Over a 2-week duration, 0.1 ml of samples were removed each day. Samples were centrifuged and resuspended in 0.1 ml of 50 mM citrate–phosphate buffer (pH 8.0) with 50 μM $CoCl_2$. OPH assays were conducted as described above.

Degradation of OPs by the engineered *P. putida* JS444

P. putida JS444 carrying pNOG33 was inoculated at $OD_{600} = 0.1$ in minimal salts medium (Spain and Nishino 1987) supplemented with 0.2 mM IPTG, 0.2 mM PNP, 0.1% yeast extract, and 50 μg ml^{-1} kanamycin and incubated at 30°C and 300 rpm until the yellow color of PNP disappeared. At this time additional PNP (0.2 mM) was added and the sequence repeated for three more times. The cells were centrifuged at 4°C, followed by washing with 50 mM citrate–phosphate buffer (pH 8.0), and resuspended in the same buffer with 50 μM $CoCl_2$. For the OP degradation test, 0.2 mM paraoxon, parathion, or methyl parathion was added to cell suspension ($OD_{600} = 3$). Samples were incubated at 30°C with shaking, taken at different time points, and measured for the residual OP concentration and PNP released from hydrolysis of OPs as described previously (Liu et al. 2007; Yang et al. 2008). Samples without inoculation were kept as controls.

Soil samples from Tsinghua University, Beijing, China, were used for this study and were never exposed to any OP compound before. The soil had a pH of 6.8 and 4.86% organic matter. Soil samples (5 kg) were sterilized by fumigation as described previously (Singh et al. 2004). Subsamples (100 g) of the fumigated and nonfumigated soil were treated under aseptic condition with parathion (100 mg kg^{-1}), respectively. One set of fumigated and nonfumigated soils in triplicate was inoculated with the engineered *P. putida* JS444 (10^6 cells g^{-1}), and another set without inoculation was kept as controls. The inoculum was thoroughly mixed into the soils under sterile condition. The soil moisture was adjusted by the addition of distilled water to 40% of its water-holding capacity. The soils were incubated at 30°C for 15 days in the dark and periodically inoculated with the engineered *P. putida* JS444. Pesticide extraction and analysis were carried out as described previously (Singh et al. 2004). PNP extraction and quantification were done as described earlier (Liu et al. 2007).

Results and discussion

Surface localization of OPH–GFP fusion in *P. putida* JS444

Both InaK from *P. syringae* KCTC1832 and InaV from *P. syringae* INA5 have been used for cell surface display of heterologous proteins (Schmid et al. 1997; Jung et al. 1998a). Even though functionally similar, there is only 77% sequence homology between the two proteins. Most of the differences occur at the critical N-terminal domain, which interacts with the phospholipids moiety of the outer membrane (Kozloff et al. 1991; Wolber 1993). In the present study, to investigate the feasibility of targeting GFP fusion onto the cell surface of *P. putida* JS444, the truncated InaV protein from *P. syringae* INA5 (Schmid et al. 1997) was used as a surface-anchoring motif. A surface expression vector, pNOG33, coding for INPNC–OPH–GFP was constructed as described above. Expression of INPNC–OPH–GFP is tightly regulated by a *tac* promoter due to the presence of the $lacI^q$ gene on the plasmid.

Expression of INPNC–OPH–GFP in *P. putida* JS444 was verified by Western blot with either OPH or GFP antiserum. A band corresponding to INPNC–OPH–GFP at 100 kDa was detected in whole-cell lysates (Fig. 1a, b, lanes 1 and 2). The localization of INPNC–OPH–GFP in the outer membrane fraction was also demonstrated by immunoblotting with either OPH or GFP antiserum (Fig. 2a, b, lanes 4 and 3).

Proteinases cannot penetrate the outer membrane and, therefore, only surface-exposed proteins could be degraded by proteinases. Pronase is a mixture of broad-specificity proteases (Li et al. 2004). A pronase accessibility assay can be used to provide evidence

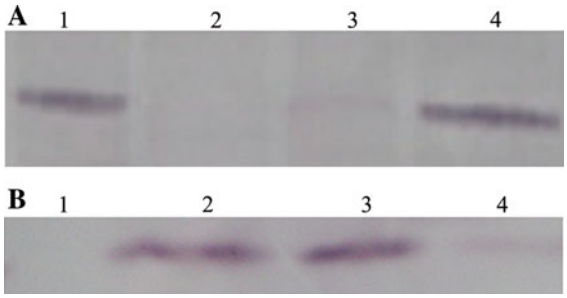

Fig. 1 Western blot analysis for subcellular localization of INPNC–OPH–GFP fusion in *P. putida* JS444 carrying pNOG33. **a** Immunoblotting of different cellular fractions with anti-OPH serum. *Lane 1* whole-cell lysates; *lane 2* negative control (JS444/pVLT33); *lane 3* soluble fraction; *lane 4* outer membrane fraction. **b** Immunoblotting of different cellular fractions with anti-GFP serum. *Lane 1* negative control (JS444/pVLT33); *lane 2* whole-cell lysates; *lane 3* outer membrane fraction; *lane 4* soluble fraction

for the surface localization of OPH–GFP. With the pronase treatment, the fluorescence for cells carrying pNOG33 decreased by 83%, while the fluorescence for cells carrying pOG33 dropped only 6%. The OPH activity for cells carrying pNOG33 decreased by 81%, while the activity for cells carrying pOG33 dropped only 6%. After the treatment of cells with pronase, no target proteins were detected in the outer membrane fraction using either OPH or GFP antiserum.

Immunolabeling with specific antibodies or antisera is an useful tool to detect surface-exposed proteins (Shi and Su 2001). To confirm the presence of INPNC–OPH–GFP on the *P. putida* surface, cells were probed with either OPH or GFP antiserum as a primary antibody and then fluorescently stained with rhodamine-labeled goat anti-rabbit IgG antibody. Since antibodies cannot diffuse through the outer membrane, specific interactions should only occur with proteins exposed on the cell surface. Under a fluorescence microscopy, cells carrying pNOG33 were brightly fluorescent (Fig. 2b, d), while cells expressing OPH–GFP intracellularly (pOG33) were not immunolabeled (Fig. 2a, c). In contrast to the control cells carrying pVLT33 (Fig. 3a), the green fluorescence was observed on the cells carrying pNOG33 (Fig. 3b). From all of these results, we concluded that OPH–GFP fusion was displayed functionally on the cell surface using the INPNC anchor InaV protein.

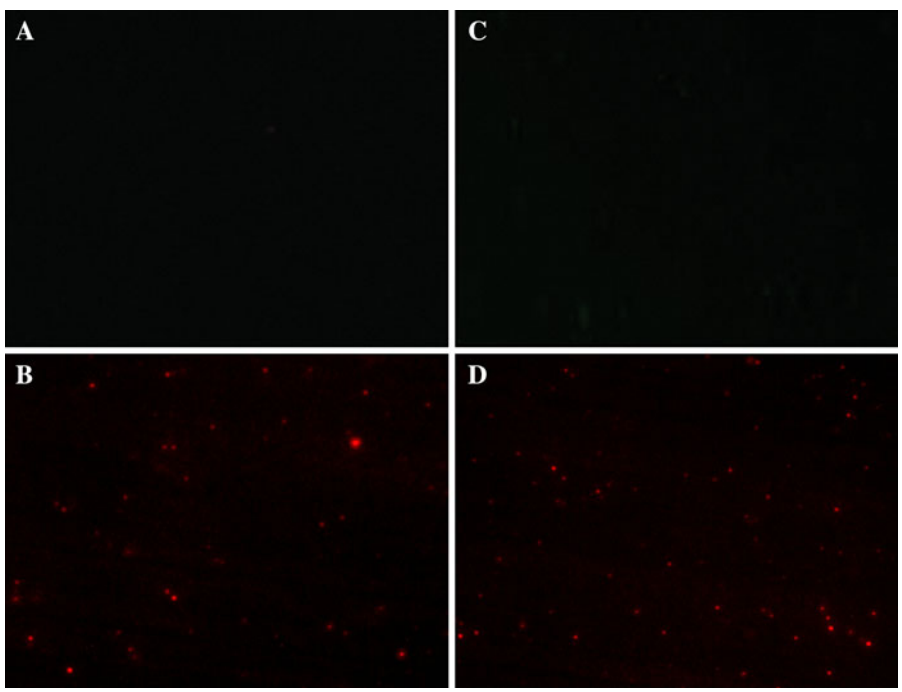

Fig. 2 Immunofluorescence micrographs of *P. putida* JS444/pOG33 (**a**, **c**) and *P. putida* JS444/pNOG33 (**b**, **d**). Cells were probed with either OPH (**a**, **b**) or GFP antiserum (**c**, **d**) and then fluorescently stained with goat anti-rabbit IgG-rhodamine conjugate

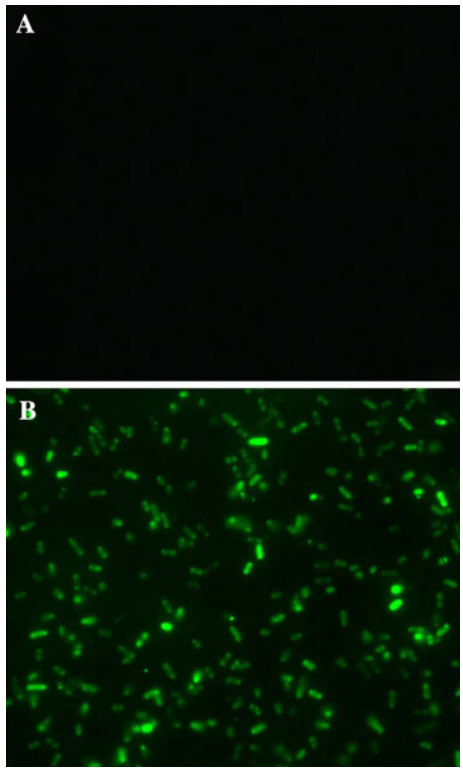

Fig. 3 Fluorescence micrographs of *P. putida* JS444/pVLT33 (**a**) and *P. putida* JS444/pNOG33 (**b**). Cells were observed by using a fluorescence microscopy equipped with FITC and Rhodamine filters

GFP is an 11-stranded β-barrel threaded by an α-helix running up the axis of the cylinder (Yang et al. 1996). So far, only a few anchoring motifs that include Lpp-OmpA from *E. coli* and INP from *P. syringae* have an ability to target GFP onto the cell surface (Shi and Su 2001; Li et al. 2004). This difficulty of surface targeting of GFP may be attributed to three-dimensional structure of GFP. The present study is the first demonstration of the functional expression of GFP on the cell surface of *Pseudomonas* species.

The broad-host-range vector, pVLT33, is an RSF1010 derivative and therefore able to replicate in a wide variety of gram-negative bacteria (de Lorenzo et al. 1993). Additionally, INP can be used for targeting enzymes or peptides onto the cell surface of indigenous microbes, such as *Moraxella* sp. (Shimazu et al. 2001b) and *Pseudomonas* sp (Lei et al. 2005; Lee et al. 2006). The pVLT33-based vector, pNOG33, could potentially be utilized for the functional display of OPH–GFP fusion on cell surfaces of indigenous microbes.

Whole-cell activity and fluorescence

The whole-cell activity of *P. putida* JS444 displaying OPH–GFP was fivefold higher than that of the same strain expressing cytosolic OPH–GFP (Fig. 4a). The physical binding between the pesticides and OPH was reinforced by expressing OPH on the *P. putida* surface, and this enhances whole-cell catalytic efficiency. Prior to IPTG induction, OPH activity was not detected and fluorescence remained at the original background level. The activity and fluorescence increased gradually after induction and reached maximums at 24 h (Table 2). The fluorescence intensity was plotted versus the OPH activity, and the fluorescence was proportional to the OPH activity over a 24-h induction (Fig. S1). Thus, GFP can be used as a fusion partner for monitoring OPH expression and activity.

Whole-cell activity in *P. putida* JS444 and in *E. coli* DH5α was compared. *P. putida* JS444 carrying pNOG33 showed twofold higher activity than *E. coli* DH5α carrying pNOG33 under the same conditions (Fig. 4a). To further investigate the efficiency of surface expression in *E. coli*, the subcellular

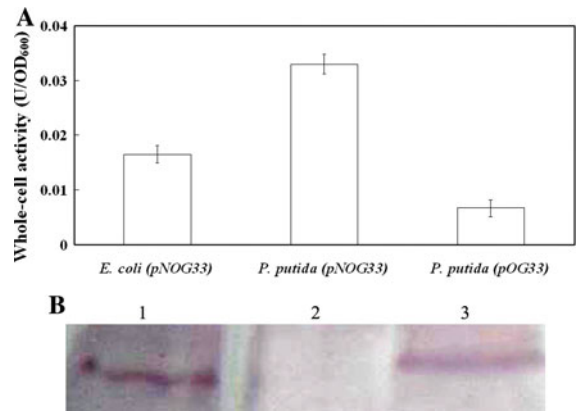

Fig. 4 **a** Whole-cell OPH activity in *E. coli* DH5α/pNOG33, *P. putida* JS444/pNOG33 and *P. putida* JS444/pOG33 cultures. Data are means $\pm$ standard deviations of three replicates. **b** Western blot analysis for subcellular localization of INPNC–OPH–GFP in *E. coli* DH5α carrying pNOG33. GFP antiserum was used at a 1:1,000 dilution. *Lane 1* soluble fraction; *lane 2* negative control (DH5α/pVLT33); *lane 3* outer membrane fraction

Table 2 Whole-cell OPH activity and GFP fluorescence assay

Post-induction (h)	OPH activity (U/OD_{600})	Fluorescence intensity
0	ND	41 ± 5
6	0.010 ± 0.0023	186 ± 12
12	0.021 ± 0.0020	387 ± 19
18	0.030 ± 0.0024	551 ± 26
24	0.032 ± 0.0026	589 ± 27

Cells carrying pNOG33 were incubated at 30°C for 24 h after induction with 0.2 mM IPTG. Samples were taken at different time points and measured for whole-cell OPH activity and GFP fluorescence. Data are means ± standard deviations of three replicates

ND not detected

localization of INPNC–OPH–GFP was determined by Western blot with anti-GFP serum. As shown in Fig. 4b, a considerable amount of the INPNC–OPH–GFP fusion was found in the soluble fraction of *E. coli* DH5α, suggesting that *P. putida* JS444 had better membrane translocation using the INP anchor than *E. coli* DH5α. This can be attributed to compatibility of the INP anchor with the membrane structure of *P. putida* JS444 since INP was originally isolated from a similar species, *P. syringae* INA5. The present study highlights the potential of *P. putida* as host strain for INP-mediated cell surface display.

When using the InaK anchor for cell surface display of GFP or chitinase, proteins could not be efficiently translocated onto the cell surface under 1 mM IPTG induction (Li et al. 2004; Wu et al. 2006). A high transcription rate can block the translocation pathway of a secretory protein, as secretion is generally the limiting step (Rodrigue et al. 1999). In this study, effects of different levels of induction on the activity and fluorescence were studied. Whole-cell activity reached a maximum (0.032 U/OD_{600}) at an IPTG concentration of 0.2 mM, and further induction resulted in a gradual decline in the activity (Fig. 5a). Because GFP fluorescence is minimally affected by the barrier effect of the cell membrane, fluorescence increased gradually with increasing concentrations of IPTG (Fig. 5b). These results suggest that induction with 0.2 mM IPTG provides an optimal balance between whole-cell activity and fluorescence.

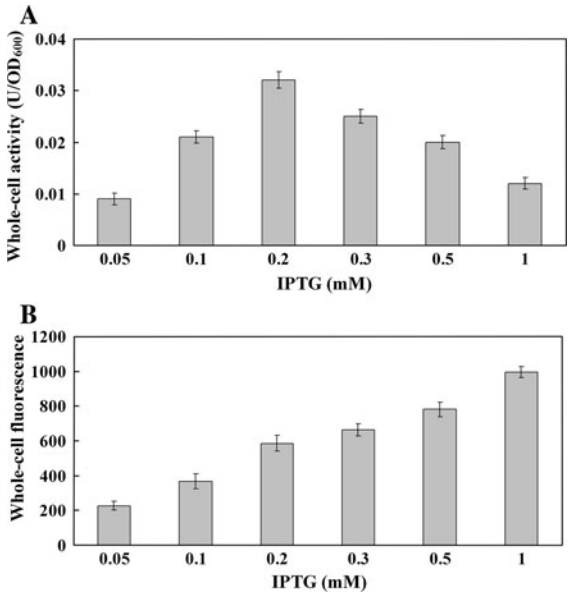

Fig. 5 Whole-cell activity (**a**) and fluorescence (**b**) of *P. putida* JS444/pNOG33 under different levels of induction. Data are means ± standard deviations of three replicates

Stability of cultures expressing INPNC–OPH–GFP

Anchorage of heterologous proteins on the cell surface may result in instability of the outer membrane and inhibition of cell growth (Samuelson et al. 2002). To test whether surface display of OPH–GFP inhibits cell growth, the growth kinetics of *P. putida* JS444 carrying pNOG33 or pVLT33 were compared. No growth inhibition was observed for cells expressing INPNC–OPH–GFP. *P. putida* JS444/pNOG33 showed the same growth profile as *P. putida* JS444/pVLT33 (Fig. 6a). The two cultures reached the same final cell density after 48 h of incubation. To monitor the stability of suspended cultures, whole-cell activity was determined periodically over a 2-week period. As shown in Fig. 6b, whole-cell activity of *P. putida* JS444/pNOG33 remained at essentially the original level over the 2-week period. These results show that surface display of OPH–GFP did not disturb the membrane structure or cause host growth defects. The stability of the cells observed here is in line with the results of previous studies in which the INP system was used for surface display of other proteins (Jung et al. 1998a, b; Shimazu et al. 2001a).

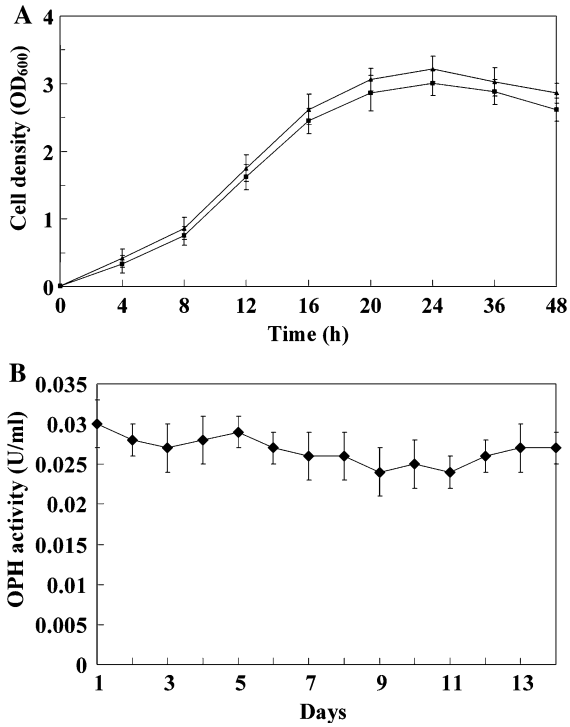

Fig. 6 **a** Time courses for the growth of *P. putida* JS444/pNOG33 (*filled square*) and *P. putida* JS444/pVLT33 (*filled diamond*). *P. putida* was incubated in Luria–Bertani (LB) medium supplemented with 50 μg/ml of kanamycin at 30°C for 4 h and then induced with 0.2 mM IPTG and incubated at 30°C for 44 h. The cell concentration was determined by measuring the optical density at 600 nm (OD_{600}) of the culture broth. **b** Whole-cell activity in suspended *P. putida* JS444 cultures with surface-expressed OPH–GFP fusion. Data are means ± standard deviations of three replicates

Degradation of OPs by the engineered *P. putida* JS444

P. putida JS444 can rapidly degrade PNP through benzoquinone, hydroquinone, maleyl acetate, and *β*-ketoadipate to tricarboxylic acid intermediates (Nishino and Spain 1993). To investigate whether the expression of OPH–GFP on the surface enabled *P. putida* JS444 to simultaneously degrade OPs and PNP, cell suspensions were incubated with 0.2 mM paraoxon, parathion, or methyl parathion. As shown in Fig. 7, paraoxon (0.2 mM) was quickly hydrolyzed within 2 h. The PNP released from hydrolysis was completely degraded within 2.5 h, indicating that the presence of OPH–GFP on the cell surface had no impact on PNP degradation. Complete hydrolysis of parathion and methyl parathion occurred within 6.5

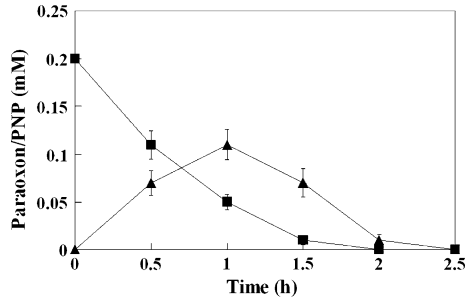

Fig. 7 Degradation of paraoxon by the engineered *P. putida* JS444 carrying pNOG33. *Filled square* paraoxon; *filled diamond* PNP released from hydrolysis of paraoxon. Data are means ± standard deviations of three replicates

and 12 h, respectively. The PNP released from hydrolysis was completely degraded within 10 and 16 h for parathion and methyl parathion, respectively (Fig. S2). In contrast, the concentration of pesticide did not change in noninoculated controls. In conclusion, PNP-substituted OPs like paraoxon could be degraded by the engineered *P. putida* JS444 via paraoxon → PNP → hydroquinone → maleyl acetate → TCA cycle.

Bioremediation, which involves the use of microbes to detoxify and degrade pollutants, has received increased attention as an effective biotechnological approach to clean up polluted environments. At present, several chemicals have been successfully removed from contaminated sites by inoculation of degrading microbes (Struthers et al. 1998; Singh et al. 2004). In this study, the addition of the engineered *P. putida* JS444 (10^6 cells g^{-1}) to fumigated and nonfumigated soils treated with 100 mg of parathion kg^{-1} resulted in a higher degradation rate than was observed in noninoculated soils. As shown in Fig. 8, parathion (100 mg kg^{-1}) was degraded completely within 15 days in fumigated and nonfumigated soils with inoculation. In contrast, <20% of the applied concentration was degraded in control fumigated and nonfumigated soils (without inoculation). Degradation patterns of parathion in fumigated soils with inoculation were similar to those of nonfumigated soils. The PNP released from hydrolysis of parathion was completely degraded within 15 days in fumigated and nonfumigated soils with inoculation (Fig. 8). The engineered *P. putida* JS444 will lose the plasmid during the cell proliferation under the non-selective conditions without antibiotics. To maintain the numbers of plasmid-bearing cells, the engineered strain

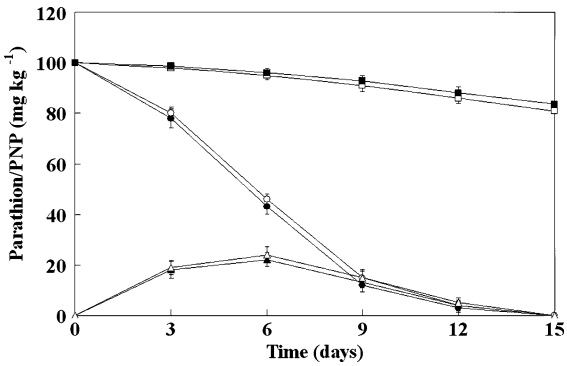

Fig. 8 Degradation of parathion in soils inoculated with the engineered *P. putida* JS444 at the rate of 10^6 cells g^{-1}. *Filled circle* fumigated soil with inoculation, parathion; *open circle* nonfumigated soil with inoculation, parathion; *filled diamond* fumigated soil with inoculation, PNP released from hydrolysis of parathion; *open rectangle* nonfumigated soil with inoculation, PNP released from hydrolysis of parathion; *filled square* fumigated soil without inoculation, parathion; *open square* nonfumigated soil without inoculation, parathion. Data are means ± standard deviations of three replicates

was periodically added to the soils during a 15-day period.

Because fluorescence can be detected by nondestructive means or high-throughput quantitative methods, GFP-marked cells are attractive biosensors (Larrainzar et al. 2005). Wild-type GFP is quenched by acidic pH values, and several of the GFP mutants are more acid sensitive than wild-type GFP. For example, 50% of the fluorescence of enhanced GFP (EGFP) quenched at pH 5.5 (Patterson et al. 1997). It was reported that surface-displayed GFP was more sensitive to extracellular pH changes than GFP residing within the cell (Shi and Su 2001). In this study, the fluorescence of JS444 cells displaying OPH–EGFP at pH 6 dropped to 45% of that at pH 7.5 and was almost entirely quenched at pH 4. In contrast, the fluorescence of JS444 cells expressing cytosolic OPH–EGFP at pH 6 maintained 90% of that at pH 7.5. Hydrolysis of OPs by OPH generates protons, leading to the decrease in the medium pH. Thus, these cells displaying OPH–EGFP have enormous potential for use as whole-cell biosensors for the rapid detection of OPs by evaluating fluorescence change as a function of OP concentration. This feasibility is currently under investigation.

Acknowledgements This work was financially supported by the 863 Hi-Tech Research and Development Program of the People's Republic of China (Nos. 2007AA06Z335 and 2009AA06A417).

References

Cha HJ, Wu CF, Valdes JJ, Rao G, Bentley WE (2000) Observations of green fluorescent protein as a fusion partner in genetically engineered *Escherichia coli*: monitoring protein expression and solubility. Biotechnol Bioeng 67:565–574

Chalfie M, Tu Y, Euskirchen G, Ward WW, Prasher DC (1994) Green fluorescent protein as a marker for gene expression. Science 263:802–805

Cormack BP, Valdivia RH, Falkow S (1996) FACS-optimized mutants of the green fluorescent protein (GFP). Gene 173:33–38

Cui ZL, Li SP, Fu GP (2001) Isolation of methyl parathion-degrading strain M6 and cloning of the methyl parathion hydrolase gene. Appl Environ Microbiol 67:4922–4925

de Lorenzo V, Eltis L, Kessler B, Timmis KN (1993) Analysis of *Pseudomonas* gene products using *lacI*^{q}/*Ptrp-lac* plasmids and transposons that confer conditional phenotypes. Gene 123:17–24

Dumas DP, Caldwell SR, Wild JR, Raushel FM (1989) Purification and properties of the phosphotriesterase from *Pseudomonas diminuta*. J Biol Chem 264:19659–19665

Elväng AM, Westerberg K, Jernberg C, Jansson JK (2001) Use of green fluorescent protein and luciferase biomarkers to monitor survival and activity of *Arthrobacter chlorophenolicus* A6 cells during degradation of 4-chlorophenol in soil. Environ Microbiol 3:32–42

Errampalli D, Leung K, Cassidy MB, Kostrzynska M, Blears M, Lee H, Trevors JT (1999) Applications of the green fluorescent protein as a molecular marker in environmental microorganisms. J Microbiol Methods 35:187–199

Horne I, Sutherland TD, Harcourt RL, Russell RJ, Oakeshott JG (2002) Identification of an *opd* (organophosphate degradation) gene in an *Agrobacterium* isolate. Appl Environ Microbiol 68:3371–3376

Jeong HS, Yoo SK, Kim EJ (2001) Cell surface display of salmobin, a thrombin-like enzyme from *Agkistrodon halys* venom on *Escherichia coli* using ice nucleation protein. Enzyme Microb Technol 28:155–160

Jung HC, Lebeault JM, Pan JG (1998a) Surface display of *Zymomonas mobilis* levansucrase by using the ice-nucleation protein of *Pseudomonas syringae*. Nat Biotechnol 16:576–580

Jung HC, Park JH, Park SH, Lebeault JM, Pan JG (1998b) Expression of carboxymethylcellulase on the surface of *Escherichia coli* using *Pseudomonas syringae* ice nucleation protein. Enzyme Microb Technol 22:348–354

Kang DG, Lim GB, Cha HJ (2005) Functional periplasmic secretion of organophosphorous hydrolase using the twin-arginine translocation pathway in *Escherichia coli*. J Biotechnol 118:379–385

Kozloff LM, Turner MA, Arellano F (1991) Formation of bacterial membrane ice-nucleation lipoglycoprotein complexes. J Bacteriol 173:6528–6536

Kwak YD, Yoo SK, Kim EJ (1999) Cell surface display of human immunodeficiency virus type 1 gp120 on

Escherichia coli by using ice nucleation protein. Clin Diagn Lab Immunol 6:499–503

Larrainzar E, O'Gara F, Morrissey JP (2005) Applications of autofluorescent proteins for in situ studies in microbial ecology. Annu Rev Microbiol 59:257–277

Lee W, Wood TK, Chen W (2006) Engineering TCE-degrading rhizobacteria for heavy metal accumulation and enhanced TCE degradation. Biotechnol Bioeng 95:399–403

Lei Y, Mulchandani A, Chen W (2005) Improved degradation of organophosphorus nerve agents and *p*-nitrophenol by *Pseudomonas putida* JS444 with surface-expressed organophosphorus hydrolase. Biotechnol Prog 21: 678–681

Li L, Kang DG, Cha HJ (2004) Functional display of foreign protein on surface of *Escherichia coli* using N-terminal domain of ice nucleation protein. Biotechnol Bioeng 85:214–221

Liu Z, Yang C, Qiao CL (2007) Biodegradation of *p*-nitrophenol and 4-chlorophenol by *Stenotrophomonas* sp. FEMS Microbiol Lett 277:150–156

Mulbry WW, Hams JF, Kearney PC, Nelson JO, McDaniel CS, Wild JR (1986) Identification of a plasmid-borne parathion hydrolase gene from *Flavobacterium* sp. by Southern hybridization with *opd* from *Pseudomonas diminuta*. Appl Environ Microbiol 51:926–930

Nishino SF, Spain JC (1993) Cell density-dependent adaption of *Pseudomonas putida* to biodegradation of *p*-nitrophenol. Environ Sci Technol 27:489–493

Patterson GH, Knobel SM, Sharif WD, Kain SR, Piston DW (1997) Use of the green fluorescent protein and its mutants in quantitative fluorescence microscopy. Biophys J 73: 2782–2790

Prosser JI (1994) Molecular marker systems for detection of genetically engineered microorganisms in the environment. Microbiology 140:5–17

Raushel FM (2002) Bacterial detoxification of organophosphate nerve agents. Curr Opin Microbiol 5:288–295

Richins RD, Kaneva I, Mulchandani A, Chen W (1997) Biodegradation of organophosphorus pesticides by surface-expressed organophosphorus hydrolase. Nat Biotechnol 15:984–987

Rodrigue A, Chanal A, Beck K, Muller M, Wu L (1999) Co-translocation of a periplasmic enzyme complex by a hitchhiker mechanism through the bacterial Tat pathway. J Biol Chem 274:13223–13228

Sambrook J, Russel DW (2001) Molecular cloning: a laboratory manual, 3rd edn. Cold Spring Harbor Laboratory Press, Cold Spring Harbor, NY

Samuelson P, Gunneriusson E, Nygren PA, Stahl S (2002) Display of proteins on bacteria. J Biotechnol 96:129–154

Schmid D, Pridmore D, Capitani G, Battistuta R, Nesser JR, Jann A (1997) Molecular organization of the ice nucleation protein InaV from *Pseudomonas syringae*. FEBS Lett 414:590–594

Serdar CM, Gibson DT (1985) Enzymatic hydrolysis of organophosphates: cloning and expression of a parathion hydrolase gene from *Pseudomonas diminuta*. Bio/Technology 3:567–571

Shi H, Su WW (2001) Display of green fluorescent protein on *Escherichia coli* cell surface. Enzym Microb Technol 28:25–34

Shimazu M, Mulchandani A, Chen W (2001a) Cell surface display of organophosphorus hydrolase using ice nucleation protein. Biotechnol Prog 17:76–80

Shimazu M, Mulchandani A, Chen W (2001b) Simultaneous degradation of organophosphorus pesticides and *p*-nitrophenol by a genetically engineered *Moraxella* sp. with surface-expressed organophosphorus hydrolase. Biotechnol Bioeng 76:318–324

Singh BK, Walker A (2006) Microbial degradation of organophosphorus compounds. FEMS Microbiol Rev 30:428–471

Singh BK, Walker A, Morgan JAW, Wright DJ (2004) Biodegradation of chlorpyrifos by *enterobacter* strain B-14 and its use in bioremediation of contaminated soils. Appl Environ Microbiol 70:4855–4863

Sogorb MA, Vilanova E, Carrera V (2004) Future application of phosphotriesterases in the prophylaxis and treatment of organophosphorus insecticide and nerve agent poisoning. Toxicol Lett 151:219–233

Spain JC, Nishino SF (1987) Degradation of 1,4-dichlorobenzene by a *Pseudomonas* sp. Appl Environ Microbiol 53:1010–1019

Struthers JK, Jayachandran K, Moorman TB (1998) Biodegradation of atrazine by *Agrobacterium radiobacter* J14a and use of this strain in bioremediation of contaminated soil. Appl Environ Microbiol 64:3368–3375

Tsien RY (1998) The green fluorescent protein. Annu Rev Biochem 67:509–544

Walker AW, Keasling JD (2002) Metabolic engineering of *Pseudomonas putida* for the utilization of parathion as a carbon and energy source. Biotechnol Bioeng 78:715–721

Wolber PK (1993) Bacterial ice nucleation. Adv Microb Physiol 34:203–237

Wu ML, Tsai CY, Chen TH (2006) Cell surface display of Chi92 on *Escherichia coli* using ice nucleation protein for improved catalytic and antifungal activity. FEMS Microbiol Lett 256:119–125

Xu JP (2006) Microbial ecology in the age of genomics and metagenomics: concepts, tools, and recent advances. Mol Ecol 15:1713–1731

Yang F, Moss LG, Phillips GN Jr (1996) The molecular structure of green fluorescent protein. Nat Biotechnol 14:1246–1251

Yang C, Liu N, Guo XM, Qiao CL (2006) Cloning of *mpd* gene from a chlorpyrifos-degrading bacterium and use of this strain in bioremediation of contaminated soil. FEMS Microbiol Lett 265:118–125

Yang C, Cai N, Dong M, Jiang H, Li JM, Qiao CL, Mulchandani A, Chen W (2008) Surface display of MPH on *Pseudomonas putida* JS444 using ice nucleation protein and its application in detoxification of organophosphates. Biotechnol Bioeng 99:30–37

Yang C, Freudl R, Qiao CL, Mulchandani A (2010) Cotranslocation of methyl parathion hydrolase to the periplasm and of organophosphorus hydrolase to the cell surface of *Escherichia coli* by the Tat pathway and ice nucleation protein display system. Appl Environ Microbiol 76:434–440

Yim SK, Jung HC, Pan JG, Kang HS, Ahn T, Yun CH (2006) Functional expression of mammalian NADPH-cytochrome P450 oxidoreductase on the cell surface of *Escherichia coli*. Protein Expr Purif 49:292–298